NanoImpact 19 (2020) 100238

Contents lists available at ScienceDirect

NanoImpact

journal homepage: www.elsevier.com/locate/nanoimpact

Research paper

The type of dietary nanoparticles influences salivary protein corona composition

Divya Srinivasan, Wut Hmone Phue, Ke Xu, Saji George*

Department of Food Science and Agricultural Chemistry, McGill University, 21111 Lakeshore Road, Sainte-Anne-de-Bellevue, QC H9X 3V9, Canada

ARTICLE INFO

Editor: Philip Demokritou

Keywords:
Nanoparticles
Dietary
Salivary proteins
Protein corona
Mass spectrometry
Salivary amylase

ABSTRACT

While nanoparticles (NPs) are copiously incorporated into different food products, the protein corona profile of saliva interacted dietary NPs and its potential influence on the function of proteins involved have received little attention. In this study the most widely used NPs such as food grade silicon dioxide (SiO_2), titanium dioxide (TiO_2) and emerging NP with application in food industry- silver (Ag) were interacted with human saliva. These particles were characterized for their physicochemical properties in their pristine state and after interacting with saliva. Analysis of the protein corona composition of saliva interacted dietary particles was carried by 1D gel electrophoresis and LC-MS/MS. We observed a net decrease in the negative surface charge and change in agglomeration size in saliva interacted NPs. Significant differences in corona composition, and protein abundance were noted among the tested particles. Several proteins with vital functions in digestion and host protections were found to be enriched on the surface of particles. In order to verify if the binding of proteins have any effect on their function, we tested the amylase and lysozyme activities of saliva in the presence and absence of NPs of SiO_2 and TiO_2. Our results showed that these particles could compromise the enzymes function wherein NPs of SiO_2 showed the highest effect. Overall, our study, identified human salivary proteins involved in the protein corona of dietary particles and showed that vital functions of saliva such as digestion and antimicrobial activities could be partially affected by protein-nanoparticle interactions in saliva.

1. Introduction

Nanoparticles (NPs) are widely applied in the cosmetic, food and nutraceutical industry for improving stability, quality, bioavailability of active ingredients and overall function of the final product (Rashidi and Khosravi-Darani, 2011; Hulla et al., 2015; Bhushan, 2017). The increasing use of NPs in food and consumer products can lead to human exposure through oral route (McCracken et al., 2016). Upon entry into human body and encounter with biological fluids, the surface of the NPs will be decorated with wide range of biomolecules- generally referred to as "corona". Surface corona plays an importance role in the biological identity of NPs that influence their fate and transport in the body (Docter et al., 2015; Ke et al., 2017). The concept of protein corona was extensively studied for plasma proteins interacted NPs because of its relevance to therapeutic interventions through injected nano-delivery systems (Barrán-Berdón et al., 2013; Tenzer et al., 2013; Winzen et al., 2015). While, daily human exposure to NPs through oral route is estimated to be 10^{12}–10^{14} (Powell et al., 2010), studies addressing the interaction of NPs with proteins of relevance to gastro-intestinal system are scarce (McCracken et al., 2016). Knowledge on the protein corona of ingested NPs is essential to understand the fate of NPs in the body and its effect on protein function.

Human saliva is a complex mixture of proteins and minerals and has several physiological roles which helps in maintaining homeostasis in the oral cavity. Saliva is constituted by secretions from multiple salivary glands and is composed of water, electrolytes, mucus, white blood cells, epithelial cells, glycoproteins, nitrogenous products, enzymes (such as amylase and lipase), antimicrobial agents such as secretory IgA and lysozyme proteins (de Almeida et al., 2008). Major functions of the human saliva are host defence, nutrient digestion and protective functions which includes tissue coating, lubrication, humidification, immunological activity, anti-(Bacterial, viral, Fungal) activity, digestive enzymes, bolus formation and taste perception (Humphrey and Williamson, 2001; de Almeida et al., 2008). The potential of NPs to interfere with vital functions of saliva is expected given the proven inhibitory action of NPs such as TiO_2 and SiO_2 on trypsin (Phue et al., 2019) and lysozyme (Vertegel et al., 2004), respectively.

In this study we investigated food grade silica (SiO_2) particles (nano and micron size), titanium dioxide (TiO_2) and citrate coated Silver (Ag) NPs to understand (1) the qualitative and quantitative differences in the

* Corresponding author.
E-mail address: saji.george@mcgill.ca (S. George).

https://doi.org/10.1016/j.impact.2020.100238
Received 9 April 2020; Received in revised form 24 June 2020; Accepted 7 July 2020
Available online 12 July 2020

protein corona of saliva interacted particles and (2) to verify if the interaction of particles with salivary enzymes (lysozyme and amylase) compromise their function. We report the difference in type and relative abundance of proteins associated with hard corona of saliva interacted particles (SiO_2 MP, SiO_2 NP, TiO_2 NP, Ag) and that dietary particles could compromise the vital functions of saliva such as digestion of starch and antimicrobial activity. To our knowledge, this is the first study reporting the interaction of dietary NPs with human saliva, which point towards potential health implications of exposure to dietary NPs.

2. Materials and methods

2.1. Materials

Bovine serum albumin (BSA), 3,5-Dinitrosalicylic acid, maltose monohydrate, soluble potato starch, Lysozyme from chicken egg white (L6876), iodoacetic acid, DDT (dichlorodiphenyltrichloroethane) and Micrococcus *lysodeikticus* ATTC no.4698 were purchased from Sigma Aldrich (St. Louis, Missouri, United States). The pierce 660 nm protein assay kit was supplied by Thermo-Fisher Scientific (Scotia court, Ontario, Canada). Sodium dodecyl sulphate -polyacrylamide gel electrophoresis (SDS-PAGE) chemicals and protein standards were purchased from Bio-Rad laboratories (Mississauga, Ontario, Canada) and Trypsin was obtained from Promega MS grade). Solvents used for LC-MS/MS orbitrap were MS grade. For all the experiments, the stock solution and buffer (PBS buffer −0.01 M, pH 7.4) were prepared according to the standard laboratory procedures using Milli-Q reagent grade water (MilliQ, Millipore, Canada).

2.2. NPs used in the study

The food grade silicon dioxide particles (SiO_2) in nano size (AEROSIL 200F) and micron size (SIPERNAT 22) were obtained from Evonik Corporation (NJ, United States). We chose food grade silica for this study, as previous studies from our group had shown that the relative abundance of branched siloxane groups (Si-O-Si) are less and linear siloxane groups are high in food grade particles compared to non-food grade particles and both grades of silica has distinguishable difference in their agglomeration behaviour (Phue et al., 2019). Titanium dioxide NP -Anatase (TiO_2) was purchased from Sigma Aldrich (St. Louis, Missouri, United States). The Citrate coated Ag NPs (Citrate-AgNPs) were synthesized according to the protocol reported earlier (Huynh and Chen, 2011). Briefly, 1 mM aqueous solution of silver nitrate with the capping agent (10 mM trisodium citrate solution) in the ratio of 2:1 was mixed together. The mixture was vortexed for 2 min and wrapped with aluminium foil and incubated in water bath for 3 h at 70 °C until the colour of the mix changed to greenish yellow. The resulting mixture was centrifuged for 30 min at 14,000 rpm and the pellets were washed twice by re-suspending in deionized water and centrifugation. Washed NP pellet was re-suspended in deionized water for further use. Pellet obtained from 5 mL of the solution containing washed NPs were freeze dried and weighed for obtaining the concentration of NPs (weight/mL).

2.3. Physical characterization

The average size, polydispersity index (PDI) and surface charge of particles were characterized by Scanning Electron Microscopy (SEM), Dynamic Light Scattering (DLS) and zeta potential measurement, respectively. The hydrodynamic diameter and the zeta potential of NPs dispersed in buffer (PBS) and saliva (Incubated for 1 h at 37 °c) were determined using a dynamic light scattering (DLS) (Nanobrook Omni instrument, Brookhaven's, New York, USA), at 25 °C at a concentration of 50 μg/mL (Deng et al., 2009; Tenzer et al., 2013). Samples prepared for the DLS were loaded into a pre-rinsed folded capillary cell for the zeta potential measurement with an applied voltage of 100 V. For SEM analysis (Hitachi, SEM-SU8230, Japan) samples (5 μL of 50 ppm NP dispersion) were dropped on the SEM stub, dried at room temperature for overnight and were examined at 50 KV accelerating voltage without coating (Phue et al., 2019).

2.4. Human saliva collection and processing

Saliva samples (unstimulated whole saliva) were obtained from healthy volunteers in accordance with a standard protocol (George and Kishen, 2007; Schipper et al., 2007) after obtaining institutional REB. To prevent the proteolytic degradation of the salivary proteins, collection tubes were placed on ice during collection. The saliva collected from each individual was vortexed for 20 s and centrifuged at 8000 rpm for 10 min to remove the debris. The clear supernatant from each tube were pooled in order to minimize inter-individual variation in saliva composition with respect to protein quality and quantity. The pooled saliva was transferred to Eppendorf tubes and centrifuged at 12,000*g* for 10 min and the supernatant was collected. Upon completion of processing, all processed saliva samples were stored at −18 °C for further analysis. The protein concentration of the saliva was quantified with the Bradford assay (Bradford dye reagent, Alfa Aesar, United States).

2.5. Preparation of saliva interacted dietary particles

Fifty microliter of NPs stock in buffer (10 mg/mL) were transferred in to the 450 μL of saliva (total volume of 500 μL at a concentration of 2 mg/mL) and incubated at 37 °C for 1 h under constant shaking at 100 rpm. An hour of incubation was chosen to ensure the dynamic equilibrium in the formation of protein corona (Tenzer et al., 2013). Saliva samples without NPs were prepared in identical way with equal volume of being buffer added instead of NPs suspension. After incubation, the particles were separated from the supernatant by centrifugation at 12,000 rpm for 30 min. The pellet was re-suspended in 500 μL of PBS buffer and centrifuged again to pellet the bound protein-particle complexes. Subsequently, the particle pellet was resuspended in PBS buffer and washed by three centrifugation steps at 12,000 rpm for 15 min and were suspended in 50 μL of SDS sample buffer (2% SDS, 5% β-mercaptoethanol, 10% glycerol and 62.5 mM Tris-HCl) (Lundqvist et al., 2008).

Due to the agglomeration in aqueous medium, the calculation of total surface area for the NPs was not practical for dosimetry. Therefore, the weight/volume was used for the dosimetry of particles (Deng et al., 2009).

2.6. Desorption of salivary proteins from dietary particles

For 1D-GE, the proteins bound to particles were eluted by boiling the particle-proteins complex with SDS sample buffer. For this, the particle-protein pellet was mixed with 50 μL of SDS sample buffer and was boiled for 5 min at 95 °C. The supernatant with desorbed proteins from the particle were separated by centrifuging at 12,000*g* for 10 min. The collected sample was used for bound protein quantification and 1D-GE. Whereas, for the proteomic analysis using LC-MS/MS, the proteins were eluted from the particles by boiling the pellet particle complex with Laemmli buffer.

2.7. Protein quantification

The amounts of proteins bound to particles were quantified after desorption of proteins from NPs using 2% SDS by Pierce 600 nm assay. Briefly, 20 μL of the sample were mixed with 200 μL of Pierce 660 nm assay reagent, incubated at room temperature for 10 min with gentle shaking and the absorbance was read at 660 nm using spectra max i3x plate reader (soft max pro 7.0.3, Molecular Devices, USA) (Winzen

et al., 2015). BSA (Sigma Albumin, Bovine) was used as a standard and blank readings were made with particles that were not interacted with saliva.

2.8. One-dimension (1D) SDS PAGE

The particles collected after the interaction with saliva were mixed with 50 μL of SDS sample buffer. We used gradient SDS-PAGE for visualizing the protein bands. For this, 20 μL of particle suspension was loaded on to a polyacrylamide gel with 4% acrylamide concentration for stacking gel and a resolving gel with gradient of acrylamide concentration of 8–12%. The gels were run using gel electrophoresis unit (Bio-Rad, model 3000xi) at a constant voltage of 50 V for 4 h. The resulting gel was stained with Coomassie brilliant blue stain followed by silver staining (Bio-Rad) with gentle agitation. A combined Coomassie blue-silver stain method was followed to increase the sensitivity of the detectable salivary proteins. All experiments were conducted in triplicates to ensure the reproducibility of the general pattern and band intensities on the 1D gels.

2.9. Protein identification by mass spectrometry

We performed LC-MS/MS mass spectrometry analysis using 3000HPLC- orbitrap fusion MS (Thermo Scientific, Canada). Briefly, the pelleted particle-protein complexes obtained from the last centrifugation step in corona preparation were re-suspended and incubated in Laemmli buffer and the protein solution (40 μL) was loaded onto a single well of a stacking gel to remove lipids, detergents and salts. Subsequently, the stacked proteins were reduced using 10 mM DTT, alkylated with iodoacetic acid and then digested with trypsin in accordance with the standard protocol for in-gel digestion (Shevchenko et al., 2007). The resulting peptides were re-solubilized in 0.1% aqueous formic acid and 2% acetonitrile and were loaded onto a Thermo Acclaim Pepmap (Thermo, 75uM ID X 2 cm C18 3uM beads) precolumn and then onto an Acclaim Pepmap Easy spray (Thermo, 75uM X 15 cm with 2uM C18 beads) analytical column separation using a Dionex Ultimate 3000 uHPLC at 220 nL/min with a gradient of 2–35% organic acid (0.1% formic acid in acetonitrile) over 2 h. Peptides were analysed using a Thermo Orbitrap Fusion mass spectrometer operating at 120,000 resolution (FWHM in MS1, 15,000 FWHM for MS/MS) with HCD sequencing of all peptides. Tandem mass spectra were extracted and deisotoped by PROTEOME DISCOVERER version 2.0. Charge state deconvolution was not performed. Scaffold (version Scaffold_4.10.0, Proteome Software Inc., Portland, OR) was used to validate MS/MS based peptide and protein identifications. The raw data were converted into *.mgf format (Mascot generic format), searched using Mascot 2.3 against human sequences (Swissport 2018). Mascot was searched with a fragment ion mass tolerance of 0.100 Da and a parent ion tolerance of 5.0 PPM. Protein probabilities were assigned by the Protein Prophet algorithm (Nesvizhskii et al., 2003). Peptide identifications were accepted if they could be established at greater than 95.0% probability by the Peptide Prophet algorithm (Keller et al., 2002) with Scaffold delta-mass correction and contained at least 2 identified peptides. Proteins were annotated with GO terms from NCBI (downloaded 8-Aug-2018) (Ashburner et al., 2000).

2.10. Data analysis using bioinformatics tools

The proteomic data from Scaffold™ was used in bioinformatic tools such as Expasy, Pantherdb, Bioinformatics.psb, perseus for the analysis of isoelectric point, gene ontology classification, Venn diagram and cluster analysis respectively. The theoretical isoelectric point for the selected list of proteins was calculated using tools available from Expasy.org (https://web.expasy.org/compute_pi/). To describe the gene function, the GO (gene ontology) data which includes molecular function, biological function, protein class were analysed using Scaffold and Panther tools (http://www.pantherdb.org/).

To identify the overlap and the unique protein gene list, we used bioinformatic webtool from Ugent (http://bioinformatics.psb.ugent.be/webtools/Venn/). The cluster analysis and statistical analysis for the genes corresponding to the identified proteins were analysed using Perseus software (http://www.biochem.mpg.de/5111810/perseus). Fold change value was calculated in Scaffold™ by comparing it with control sample (Human Saliva) and the Z score for all the genes with fold change ≥ 2 were calculated in Perseus software for cluster analysis.

2.11. α-Amylase enzyme activity by DNS assay

The α-amylase activity was measured in the presence of SiO_2 and TiO_2 particles at a concentration of 2 mg/mL of particles in whole human saliva. Saliva without particle was considered as control. Briefly, the effect of particle on α-amylase activity was studied by incubating the saliva (180 μL) and particle (20 μL) at a concentration of 2 mg/mL for 1 h. The substrate was mixed with 1% NaCl in the ratio of (4:1) and incubated at 37 °C for 5–10 min to equilibrate the reaction mixture. Subsequently, 0.2 mL of the substrate (1% soluble potato starch) was added into the saliva -particle mixture and incubated for 5 min followed by addition of 0.2 mL of DNS reagent (dye) and place it in a heating block for 15 min. After boiling, the Eppendorf tubes were cooled in ice bath and were added with 0.9 mL of deionized water. The tubes were centrifuged at 12,000 rpm for 10 min to pull down the particles and 200 μL of each of the sample was pipetted in the microplate and the absorbance was read at 540 nm. The released sugar in the test sample and control was calculated and compared. All experiments were performed at least three times with triplicate samples.

2.12. Turbidimetric assay for lysozyme activity

Turbidimetric assay based on the lysis of gram-positive *Micrococcus lysodeikticus* bacterial cells was used for the measurement of the salivary lysozyme activity (Helal and Melzig, 2008). For this, the substrate (freeze dried bacterial cells) was prepared at a concentration of 0.30 mg/mL using phosphate buffer. The test sample containing 30 μL of saliva and 30 μL of dietary particles (2.0 mg/mL) were pre-incubated for 1 h in 96 well plate. The wells were then added with 170 μL of substrate solution (bacterial cell suspension). The mixture was incubated for additional 5 min before the absorbance was read at 450 nm using a plate reader. Thirty microliter of saliva sample added with 30 μL PBS buffer served as the control. All experiments were repeated 3 times with triplicate sample in each test.

3. Results

3.1. Dietary particles characterization

The dietary particles used in this experiment were characterized prior to their interaction with human saliva to assess their size, shape, hydrodynamic diameter and surface charge (ζ potential). Particle characterization were performed in MQ water, PBS buffer and whole saliva by using scanning electron microscopy (SEM), dynamic light scattering (DLS) and zeta potential measurements as shown in Table 1 and Fig. 1. According to the suppliers, the primary particles sizes of SiO_2 NP, SiO_2 MP and TiO_2 NPs were 12 nm, 110 μm and $\sim < 44$ μm, respectively. However, SEM analysis showed that size of primary particles constituting the aggregates are 25 nm, 70 nm, 150 nm and 50 nm for SiO_2 NP, SiO_2 MP, TiO_2 NP and Ag NP respectively, which are largely in agreement with the data supplied by the supplier except for SiO_2 MPs (Fig. 1). In the case of Ag NPs, we noticed the presence of rod-shaped silver nanoparticles although majority of them were spherical in shape (Fig. 1D).

All particles agglomerated to certain extent in saliva, except for SiO_2 NPs which was comparable to the size of particles dispersed in water. A

Table 1
Summary of physical characterization of the dietary particles used in the experiment. Effective diameter by number in (nm); Poly dispersity index-PDI; and Zeta potential (ZP) in mV of all the four dietary particles measured when dispersed in buffer and human whole saliva incubated for 1 h at 37 °C. Values are mean ± SD from three independent experiments.

Dietary particles	Suspended in water			Suspended in PBS buffer			Suspended in whole saliva		
	Effective diameter by number (nm)	PDI	Zeta Potential (mV)	Effective diameter by number (nm)	PDI	Zeta Potential (mV)	Effective diameter by number (nm)	PDI	Zeta Potential (mV)
SiO_2 NP	50.53 ± 15.10	0.32 ± 0.082	−25.95 ± 0.788	55.62 ± 16.94	0.37 ± 0.20	−26.47 ± 5.62	27.43 ± 4.56	0.28 ± 0.01	−20.05 ± 1.61
SiO_2 MP	41.78 ± 4.05	0.34 ± 0.11	−20.13 ± 2.63	41.96 ± 24.10	0.25 ± 0.03	−28.54 ± 2.76	235.59 ± 100.41	0.54 ± 0.34	−17.77 ± 0.96
TiO_2 NP	422.86 ± 13.41	0.13 ± 0.014	−32.61 ± 0.92	321.7 ± 173.49	0.72 ± 0.02	−43.14 ± 2.90	291.76 ± 384.43	0.20 ± 0.07	−13.67 ± 0.79
Ag NP	57.06 ± 7.57	0.50 ± 0.08	−20.40 ± 5.01	54.44 ± 9.92	0.42 ± 0.14	−10.61 ± 2.92	26.97 ± 5.13	0.362 ± 0.02	−14.33 ± 3.81

significant increase in particle size was observed for TiO_2 and Ag NPs due to the agglomeration in PBS buffer and saliva (> 100 nm). The polydispersity index (PDI) value found to be higher in PBS and lower in saliva for all the particles except SiO_2 MPs. None of the particles had a PDI value less than 0.05 suggesting that these particles were not monodispersed. All these particles exhibited negative zeta potential in PBS and saliva. The zeta potential value for all the particles in saliva showed a decrease in the net negative zeta potential (Table 1). TiO_2 NPs showed significant decrease from the initial negative charge −43.14 mV to −13.1 mV.

3.2. Protein quantification and analysis by 1D gel electrophoresis

Fig. 2(A) shows the amount of proteins bound onto the surface of particles. The total amount of adsorbed protein was significantly higher in SiO_2 NPs in comparison to TiO_2 and Ag NPs, and SiO_2 MPs. The data suggested 20–40% depletion of total proteins from saliva when particles are interacted at a concentration likely to be encountered during consumption of food commodities contain manufactured NPs.

Fig. 2(B) shows 1D-PAGE of salivary proteins retrieved from the pellet of dietary particles incubated in human saliva for 1 h (lane 3–6) and proteins from human whole saliva (lane 2). The difference in band intensities suggested differences in the relative abundance of proteins in tested particles. As such NPs of SiO_2 showed the highest number of protein bands and the bands were darker in comparison to protein bands obtained from other particles. The enrichment of proteins on the surface of particles was observed as new bands (red box in Fig. 2(B)) which were absent in the control lane 2 (human saliva).

3.3. Proteomic profiling of salivary coronal proteins by mass spectrometry analysis

The profile of protein coronas on the surface of the dietary particles after 1 h of incubation in human saliva were investigated using LC-MS/MS. A total of 737 unique salivary proteins were identified, in which 498 were identical to the whole saliva and the remaining 239 proteins were unique to saliva interacted particles suggesting possible enrichment of specific proteins on the surface of particles. The detailed list of the identified salivary coronal proteins is provided in the supplementary data (Table S1).

The difference in the composition of the salivary protein corona around the dietary particles is evident from the Venn diagram shown in Fig. 3(A), total of 339, 372, 246, and 149 salivary proteins were identified in the coronas on SiO_2 NPs, SiO_2 MPs, TiO_2 NPs and Ag NPs, respectively (Fig. 3(A)). It was found that 123 proteins were common to all the particles surface irrespective of the size and chemistry. Number of distinct proteins present in the coronas of SiO_2 NPs, TiO_2 NPs and Ag NPs were 115, 31 and 9, respectively (Fig. 3(B)).

The relative abundance of the proteins is illustrated in Fig. 4(A) as a heap map. Hierarchical cluster analysis showed a significant difference in the abundance of proteins present on different particles. Based on GO analysis, genes corresponding to proteins could be clustered in to 5 categories. Cluster 1 has 14 genes, most of which are highly abundant in SiO_2 NPs followed by Ag NPs while, almost none with TiO_2 NPs. Cluster 2 represent genes that are significantly abundant on Ag NPs but with minimal presence on TiO_2 and SiO_2 NPs. Cluster 3 represents genes of protein that are mainly abundant on TiO_2 NPs. Similarly, cluster 4 grouped genes of proteins that are mainly abundant on SiO_2 MPs and some of the protein genes from this cluster were also found on SiO_2 and TiO_2 NPs. The last class of the cluster grouped the genes of protein that are highly abundant on the surface of SiO_2 NPs. The list of genes constituting the clusters in 4A is provided in Table S1. Fig. 4(B) represents the fold enrichment of the salivary proteins on the particles surface. We observed a significant enrichment of salivary proteins on particle surface which were close to or below the detection limit in the whole saliva. Overall, 168, 131, 80 and 72 protein genes found to be

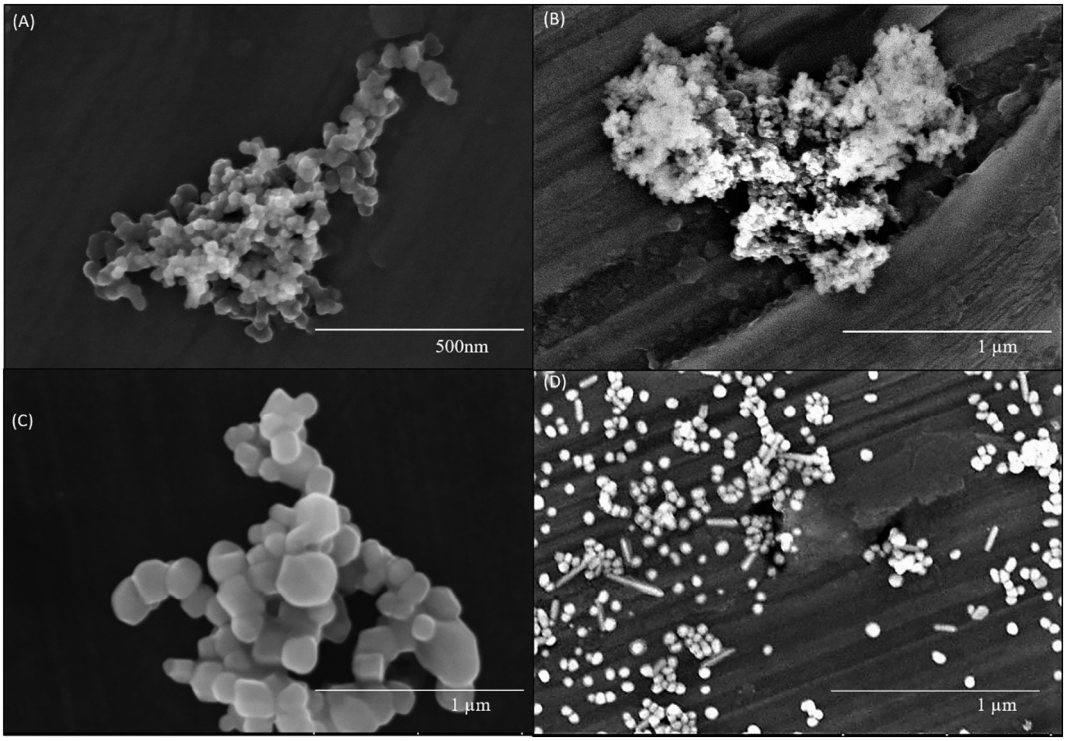

Fig. 1. SEM image of dietary particles obtained after drying the NP dispersion (50 ppm) on the SEM stub. (A) SiO_2 NP; (b) SiO_2 MP; (C) TiO_2 NP; (D) Ag NP.

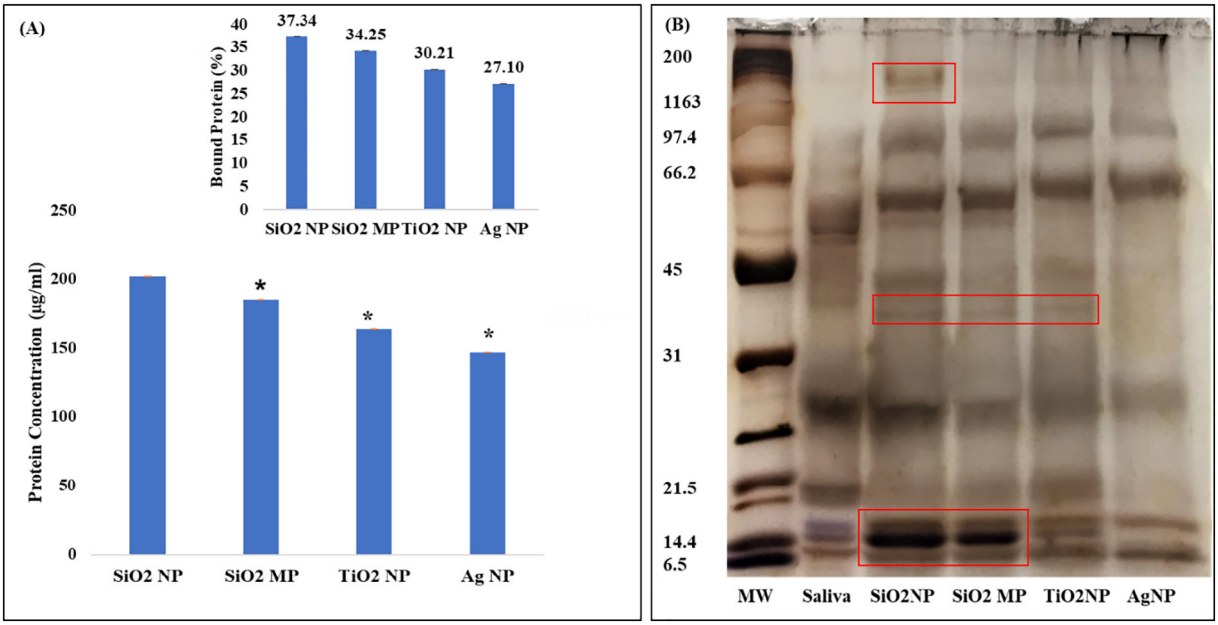

Fig. 2. Analysis of protein corona after incubation with human saliva. (A) Quantitative analysis of bound protein concentration in µg/mg of Particles: Proteins were quantified by Pierce 660 nm Assay after the desorption of proteins from particles using 2% SDS; (B) changes in the bound protein pattern of whole saliva interacted with 4 different dietary particles: Particle bound proteins were separated in 1-D SDS-PAGE and visualized by combination of Coomassie and silver staining. The Molecular Weight (KDa) of reference proteins are shown in the first lane. * Indicate statistically significant difference from SiO2NPs ($p \leq 0.05$).

significantly enriched on the dietary particles of SiO_2 NP, SiO_2 MP, TiO_2 NP and Ag NP respectively with fold enrichment of ≥ 2. The heatmap displaying fold enrichment was clustered in to 5 groups. Each cluster represents a unique pattern of protein enrichment in respective particle. Cluster 4 was found to be the major cluster with 118 protein which are constituted by either less abundant high affinity or high abundant high affinity proteins of saliva. For instance, lysozyme and lactoferrin were high abundant proteins that showed higher affinity for SiO_2 NPs and SiO_2 MPs with 3.6 & 3.2-fold enrichment from the human saliva. On the other hand, Annexin is a low abundant protein in saliva which was found to be enriched ~5.5-fold by all the tested particles.

Apolipoproteins B-100, Annexin A2 and Annexin A11 were found to be enriched by all the particles. Notably, Ag NPs showed higher value of fold enrichment for Annexin proteins. On the other hand, SiO_2 NPs showed unique pattern of fold enrichment by adsorbing almost 11 unique proteins from the list of 20 most enriched proteins

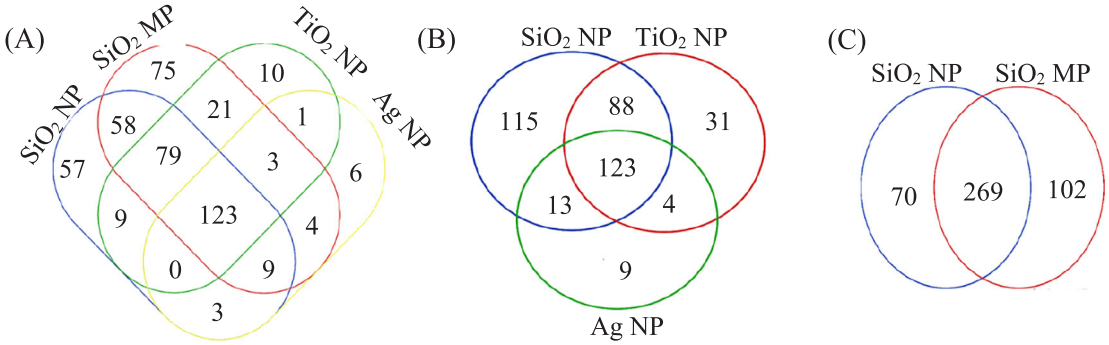

Fig. 3. Venn diagram shows the number of salivary proteins found associated with surface corona of saliva interacted particles. (A) Four dietary particles (B) only dietary NPs and (C) silica particles of micron and nano size. Distinct composition of corona associated proteins for each particle is evidenced as difference in the number of proteins and identification of unique proteins in saliva interacted particles suggested the preferential enrichment of low abundant proteins (which were not originally detected in saliva).

(Supplementary data: Table S2). Notably, only 8 proteins from the list of 20 most abundant proteins were shared by both SiO_2 NPs and SiO_2 MPs, suggesting the potential role of particle size in determining the types of proteins binding onto particles.

3.4. Comparative analysis of the protein corona on dietary particles

The top twenty most abundant salivary proteins from the protein corona formed on the 4 different dietary particles is listed in Table 2. Generally, there was high redundancy in proteins present on the corona of particles (Table 2, bold and italics). However, there were proteins that were unique for each particle.

Most abundant proteins included α-amylase-1, polymeric immunoglobulin receptor, prolactin inducible proteins, zymogen granule protein 16 homolog B, lactotransferrin, immunoglobulin constant alpha 1, alpha- 2 heavy chain, and BPI fold containing family A member 2. The difference among particles in protein abundance is exemplified by the presence of Annexin A1 and A6 exclusively in Ag NPs while proteins such as Lysozyme C, Cystatin-SN was present in all group except Ag NPs. We also compared the abundance of proteins in saliva and particle corona after emPAI optimization of spectral count to mitigate the disparity in spectral count arising from differences in number of peptides from larger and small proteins (Ishihama et al., 2005). While there was a high overlap between the list of proteins generated by these two methods, the relative ranking changed and proteins of smaller MW were seen climbing up in the ranking after emPAI optimization (Table S3).

To characterize and compare the nature of proteins that are found in the top 20 abundant and enriched proteins on the particles surface, we grouped proteins for their molecular weight (MW) and isoelectric point (pI). Almost 70% of the corona proteins were composed of those with molecular weight < 60 kDa. Unlike other particles, Ag NPs had less proteins with mass < 20 kDa and also had proteins with mass of 100–150 kDa (Fig. 5(A)). We also compared the molecular weight and pI of most enriched proteins. Mostly, the enriched proteins on SiO_2 and TiO_2 particles had MW of 100–150 KDa (Fig. 5(B)). Fig. 5(C & D) represents the protein classification by pI for abundant and enriched coronal proteins of the dietary particles, respectively. Generally, 90% of the most abundant proteins present on the particles had their pI values less than 7 (Fig. 5(C)). Notably, 50% of proteins enriched on SiO_2 NPs were with a pI value in the range of 7–11 (Fig. 5(D)).

3.5. Functional annotation of the salivary protein corona

We employed bioinformatics tools, such as Scaffold gene ontology (GO) and Panther database to classify the coronal proteins based on GO terms. Classes of proteins identified through GO term annotation are presented as stacked bar plot in Fig. 6. Enzyme modulator, hydrolase, proteins involved in host defence and immunity, signalling molecule, oxidoreductase and cytoskeletal proteins constituted ~60% of the coronal proteins. There were quantitative differences in the relative distribution of these protein classes among the tested particles. For instance, there was a two-fold increase in oxidoreductase class of proteins on Ag NPs while, the presence of oxidoreductase in other particles were comparable to that of saliva. Similarly, transcription factors were found only in SiO_2 particles. Other protein classes such as transporter, calcium binding, and carrier protein were found in higher percentage on the tested particles compared to the whole saliva which in turn suggest the enrichment of these protein classes on the surface of particles.

3.6. Influence of dietary particles on the enzyme activities of α-amylase and lysozyme in human saliva

As the NP surface have the ability to modify the structure and therefore the function of the proteins, we hypothesized that activity of α-amylase and lysozyme will be influenced by the presence of dietary particles in human saliva. All the tested particles showed statistically significant decrease in α-amylase activity as shown in Fig. 7A. Among the three dietary particles tested (SiO_2 NP, SiO_2 MP and TiO_2 NP), SiO_2 NPs exhibited the highest inhibition which was 34.94% in comparison to α-amylase activity in whole saliva (inlet Fig. 7A). SiO_2 MPs and TiO_2 NPs didn't show significant difference between them in the enzyme inhibition activity as shown in the figure inset 7A. The lysozyme function in saliva was found to be affected by the presence of SiO_2 particles (both NPs and MPs) but not by TiO_2 NPs (Fig. 7(B)). The % inhibition of lysozyme activity was 24.3, 11.58 for SiO2 NPs and SiO2 MPs, respectively (inlet, Fig. 7B).

4. Discussion

We assessed the corona protein profile of dietary particles interacted human saliva, as mouth is the port of entry for particles used in food additives, dental materials and drug formulations. Our results showed qualitative and quantitative difference in the distribution of proteins present in the hard corona of different types of dietary particles tested. NPs of SiO_2 showed the highest amount of proteins adsorbed in comparison to other particles. Proteomic analysis showed the distinct type of gene clusters corresponding to proteins adsorbed on different particles. The functional annotation of proteins found associated with particles showed higher prevalence for those involved in metabolic and defence functions.

Inorganic particles used as food additives could get released from the food matrix and could interact with saliva during mastication of food. Saliva serves pivotal function in enabling the smooth passage of food through digestive tract and is a major reservoir of digestive

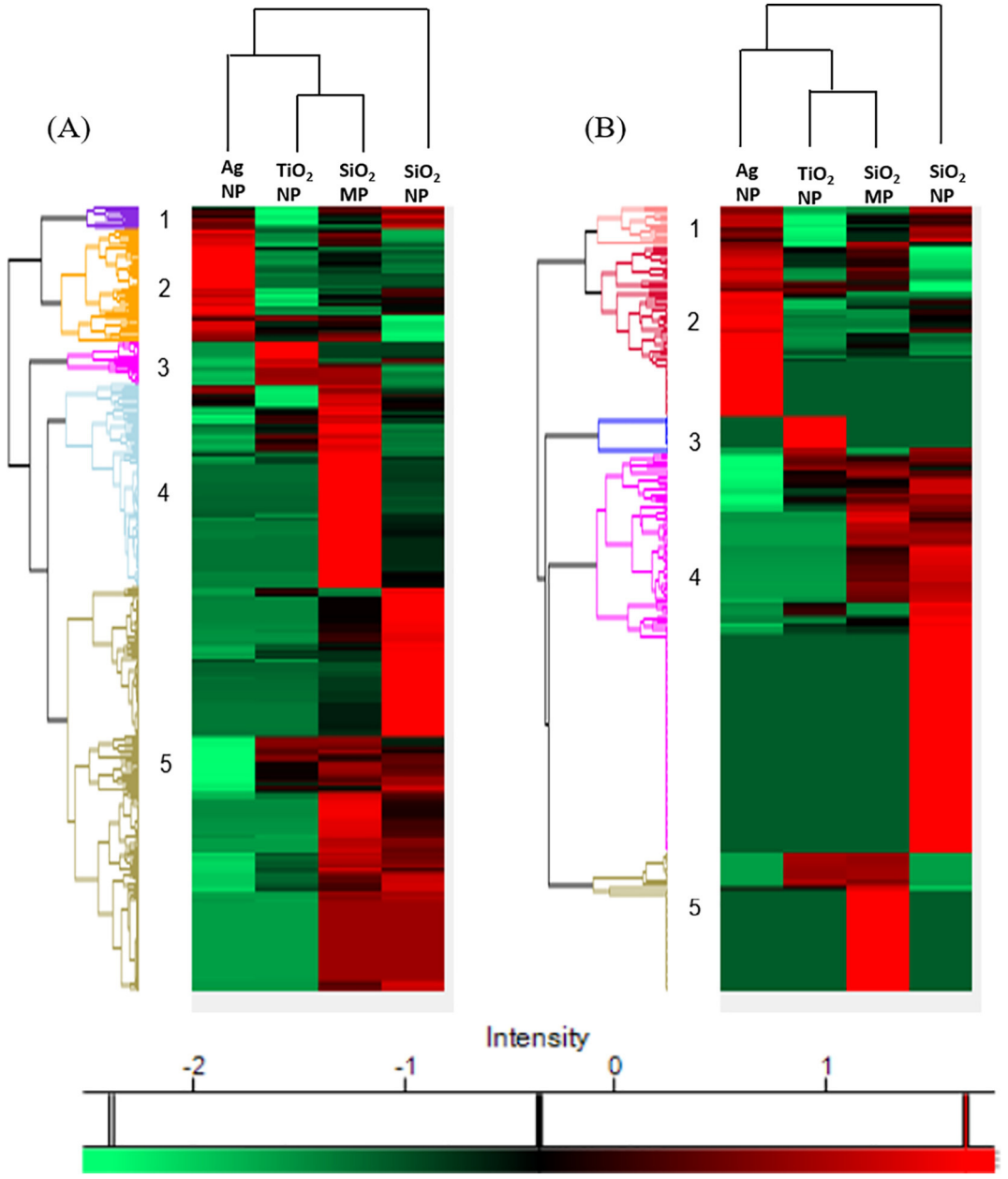

Fig. 4. Hierarchical clustering of the proteins found on the surface corona of saliva interacted dietary particles. (A) Heat map showing relative abundance of 506 differentially expressed genes corresponding to proteins identified on each dietary particle compared with human saliva. Color scheme is based on the z score values of fold change of individual proteins compared with whole saliva. (4B): Heat map showing enrichment of proteins on each dietary particle in comparison with those identified from human saliva.

enzymes and proteins of relevance to oral hygiene (Loo et al., 2010; van't Hof et al., 2014). Therefore, it is crucial to understand the interactions of human salivary proteins with particles, including NPs that are used as food additives.

We observed agglomeration of particles when they were dispersed in saliva and PBS buffer. The increase in particle size when dispersed in saliva could be explained by the combined effect of the protein corona formation and the agglomeration of the particles due to the pH and ionic strength of the saliva (Bihari et al., 2008). Many studies have shown that protein corona could stabilize the particles in the solution (Deng et al., 2009; Monopoli et al., 2011). For instance, TiO_2 and Ag NPs dispersed in water and PBS quickly agglomerate from their original size of 20 to 50 nm to hundreds of nanometres while, in the human saliva the protein coating prevents the particles from forming large clusters. The net negative charge of particles reduced after incubation in saliva, suggesting the presence of protein corona. Several studies addressing the interaction of serum plasma with NPs have showed that these physicochemical properties of the particles such as chemical composition of the particle, surface charge, surface chemistry and size, have significant influence on the formation and composition of protein corona (Docter et al., 2015; Zanganeh et al., 2018). Thus, while the main reason for the differences among particles for corona protein profile as observed in our study could be attributed to the chemical makeup of particles (including its surface chemistry and dissolution), the influence of size on the relative abundance of proteins cannot be discarded. For instance, the silica particles of comparative surface chemistry showed 269 shared proteins while 70 and 102 proteins were unique to NPs and MPs, respectively. It should be noted that the type and relative abundance of proteins bound onto NP surface are determined not only by the physicochemical properties of NPs but also the

Table 2
Twenty most abundant proteins identified in the protein corona of each dietary particle following 1 h of incubation with human saliva. Common proteins identified are highlighted in bold and italicized and unique ones in bold.

S.no	Whole saliva	SiO_2 NP	SiO_2 MP	TiO_2 NP	Ag NP
1	***Alpha-amylase 1***	Lysozyme C	***Lactotransferrin***	***Zymogen granule protein 16 homolog B***	***Zymogen granule protein 16 homolog B***
2	**Polymeric immunoglobulin receptor**	***Lactotransferrin***	***Alpha-amylase 1***	***Lactotransferrin***	***BPI fold-containing family A member 2***
3	***Prolactin-inducible protein***	*Myeloperoxidase*	***Zymogen granule protein 16 homolog B***	***Prolactin-inducible protein***	***Immunoglobulin heavy constant mu***
4	Serum albumin	***Polymeric immunoglobulin receptor***	***Polymeric immunoglobulin receptor***	***Alpha-amylase 1***	BPI fold-containing family B member 1
5	Cystatin-SN	***Prolactin-inducible protein***	Lysozyme C	***Polymeric immunoglobulin receptor***	***Polymeric immunoglobulin receptor***
6	***Zymogen granule protein 16 homolog B***	**Antileukoproteinase**	***Prolactin-inducible protein***	Lysozyme C	Myeloperoxidase
7	***Immunoglobulin heavy constant alpha 1***	Mucin-5B	***Immunoglobulin heavy constant mu***	***Immunoglobulin heavy constant mu***	Actin, cytoplasmic 1
8	Mucin-5B	Deleted in malignant brain tumors 1 protein	Mucin-5B	Myeloperoxidase	***Alpha-amylase 1***
9	***Lactotransferrin***	***Immunoglobulin heavy constant alpha 1***	Serum albumin	***BPI fold-containing family A member 2***	***Immunoglobulin heavy constant alpha 1***
10	Lysozyme C	Lactoperoxidase	Cystatin-SN	Immunoglobulin kappa constant	Carbonic anhydrase 6
11	Cystatin-S	***Zymogen granule protein 16 homolog B***	Lactoperoxidase	***Immunoglobulin heavy constant alpha 1***	Alpha-actinin-4
12	Immunoglobulin kappa constant	***Alpha-amylase 1***	***Immunoglobulin heavy constant mu***	***Immunoglobulin kappa light chain***	Apolipoprotein B-100
13	***Immunoglobulin kappa light chain***	***Immunoglobulin heavy constant mu***	***Immunoglobulin kappa light chain***	***Immunoglobulin alpha-2 heavy chain***	Annexin A1
14	***Immunoglobulin alpha-2 heavy chain***	**Protein S100-A9**	***BPI fold-containing family A member 2***	Carbonic anhydrase 6	Protein disulfide-isomerase
15	Cystatin-SA	***BPI fold-containing family A member 2***	***Immunoglobulin alpha-2 heavy chain***	BPI fold-containing family B member 1	Annexin A6
16	**Immunoglobulin heavy constant mu**	***Immunoglobulin kappa light chain***	Myeloperoxidase	Cystatin-SN	***Immunoglobulin alpha-2 heavy chain***
17	Carbonic anhydrase 6	Cystatin-SN	Cystatin-S	Lactoperoxidase	***Immunoglobulin kappa light chain***
18	***BPI fold-containing family A member 2***	Actin, cytoplasmic 1	Immunoglobulin kappa constant	Apolipoprotein B-100	Protein-glutamine gamma-glutamyltransferase E
19	Lactoperoxidase	Pyruvate kinase PKM	Deleted in malignant brain tumors 1 protein	Deleted in malignant brain tumors 1 protein	***Lactotransferrin***
20	Zinc-alpha-2-glycoprotein	***Immunoglobulin alpha-2 heavy chain***	Carbonic anhydrase 6	Actin, cytoplasmic 1	***Prolactin-inducible protein***

properties of proteins in the biological fluid along with the micro-environment.

1D gel analysis of proteins associated with particle corona showed unique bands which were absent in the saliva control pointing towards the possibility of selective enrichment of certain proteins on particle surfaces. This was further strengthened by the LC-MS/MS data. For instance, when the highly abundant mucin proteins where absent on Ag NPs, low abundant proteins such as lysozyme and lactoperoxidase were found to be enriched on Ag NPs. Apo-B100 lipoprotein, for example, showed significant enrichment on AgNPs with 64-fold increase in comparison to saliva while it was 47 and 33-fold increase in the case of SiO_2 NPs and TiO_2 respectively which are congruent with other reported studies (Jeon et al., 2011; Sanfins et al., 2011; Tenzer et al., 2011). Similarly, Annexin A2, A11, A6 were found to be enriched on TiO_2 and Ag NPs. Studies have shown that particles with negative surface charge preferentially bind with proteins with net positive charge (Karmali and Simberg, 2011; Deng et al., 2012; Tenzer et al., 2013). Accordingly, we also noticed that low abundant antimicrobial proteins displaying a positive charge (pI > 7) such as Antileukoproteinase, myeloperoxidase, Lactotransferrin and lysozyme getting enriched on these particles with net negative charge. Interestingly, particles also showed a high prevalence of proteins with net negative charge in their corona. We attribute this preferential binding of negatively charged proteins on to the surface of negatively charged particles to Vroman's effect. According to Vroman's effect the initial binding of positively charged salivary proteins mask the negative surface of particles whereby allowing the binding of negatively charged proteins. Thus, while coulombic interactions play a major role in determining protein-particle interactions, studies have also shown metal specific binding of proteins. For instance, TiO_2 particles have shown to enrich phosphoproteins such as acidic PRPs (proline rich proteins), statherin, histatin-1, cystatins S and SA-III (Salih et al., 2010). Similarly, we also observed an enrichment of proteins such as salivary proline-rich proteins, tubulin beta chain, deleted in malignant brain tumors 1 protein, fibrinogen gamma chain and collagen alpha −2(VI) on the surfaces of TiO_2 and SiO_2 particles. Another example for preferred binding of proteins on to metal surface was the enrichment of oxidoreductase on Ag NPs. Thiol group of cysteine molecules present in the active site of oxidoreductase is thought to mediate this preferred binding with AgNPs (George et al., 2012).

Generally, proteins associated with corona were identified to be majorly involved in cellular process & cell communication, metabolic process and response to stimulus. Almost 50% of enriched proteins on SiO_2 NPs are involved in catalytic activity such as transferase, hydrolase and enzyme regulator activity. As for Ag NPs the top enriched proteins are those involved mostly in hydrolase activity (33%). 67% of the proteins found on TiO_2 NPs are those involved in cytoskeletal protein binding. Another major class of proteins found enriched on particle surfaces was apolipoproteins such as Apo B100, Apo AI, Apo E. The consequence of depleting Apolipoproteins from human saliva warrants further investigation, as these proteins play a major role in lipid metabolism.

Proteins adsorbed on to the surface of the particles may undergo structural rearrangement leading to conformational changes that will render the protein to become dysfunctional due to change in the secondary structure (Phue et al., 2019; Walkey and Chan, 2012; Treuel, 2013). Particles of SiO_2 (NPs and MPs), and TiO_2 NP caused partial inhibition of α-amylase and lysozyme activity of saliva. Among the tested particles SiO_2 NPs showed the highest percentage of inhibition. Generally, silica surfaces are regarded amenable for enzyme immobilization since silica surface chemistry has little effect on proteins. Therefore, the observed loss of enzyme activity when they were interacted with SiO_2 NPs is thought to be mediated by unique interaction of NPs of SiO_2, to cause conformational change in enzyme.

Digestion of amylose and amylopectin in the mouth is often assumed to be of minimal importance, as food stays in the mouth only for

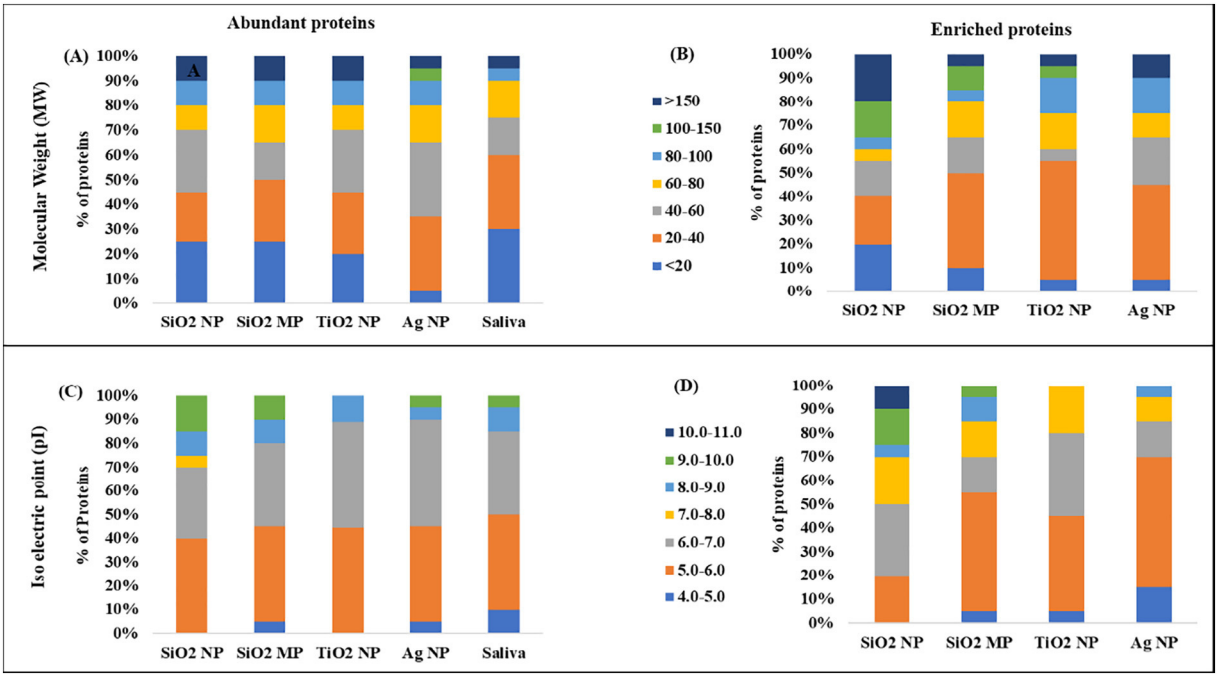

Fig. 5. Comparison of top 20 abundant (A & C) and enriched proteins (B & D) on the corona profiles based on MW & pI. A & B shows the classification of coronal proteins according to their molecular weight (MW); C&D shows the difference between abundant and enriched coronal profiles on the particles based on the calculated isoelectric point (pI).

few seconds and the time given to the enzyme to act enzymatically in the mouth during mastication vary with individuals. However, studies have shown that considerable amount of starch hydrolysis happens in mouth during mastication of food and that salivary amylase are protected from the acid inactivation in the stomach by partially digested starch (Hoebler et al., 1998; Mandel and Breslin, 2012). Therefore, binding of α -amylase to NPs of SiO_2 could compromise the action of α -amylase beyond the oral cavity. Further, the presence of NPs in small intestine could have similar effect on pancreatic α-amylase. In short, our studies showed the selective enrichment of certain proteins including digestive enzymes and that these interactions could compromise enzyme activities. The mechanism of enzyme inactivation by SiO_2 NPs is currently addressed in a separate study.

For the first time we captured the interaction of salivary proteome with dietary particles through a qualitative and quantitative approach. We observed a distinctive difference between each dietary particle on its protein corona composition with differential abundance and fold enrichment of significant salivary proteins. Further, we show that the

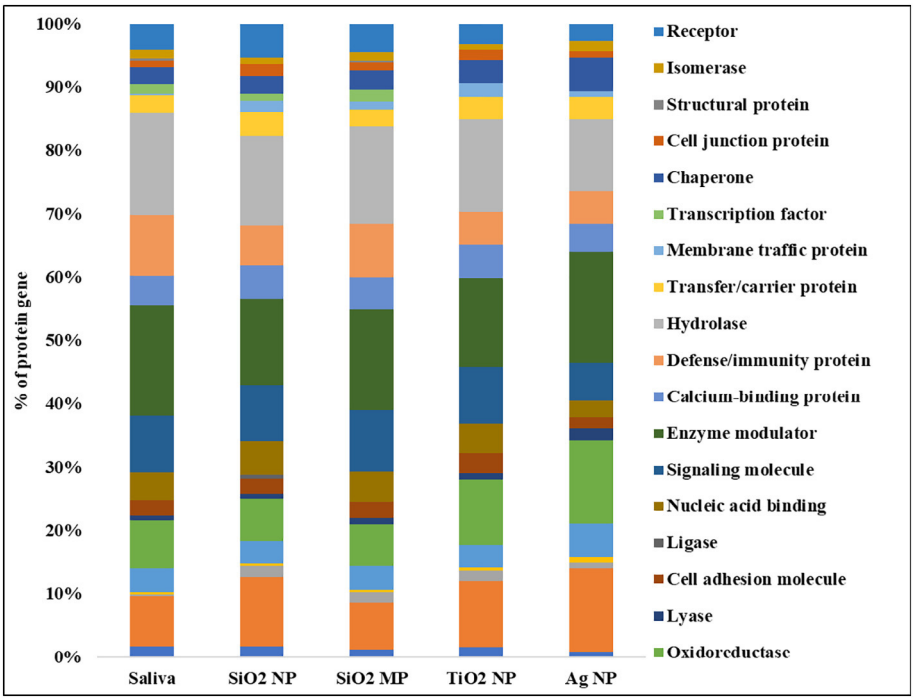

Fig. 6. Classification of proteins associated with surface corona of saliva interacted particles according to protein class.

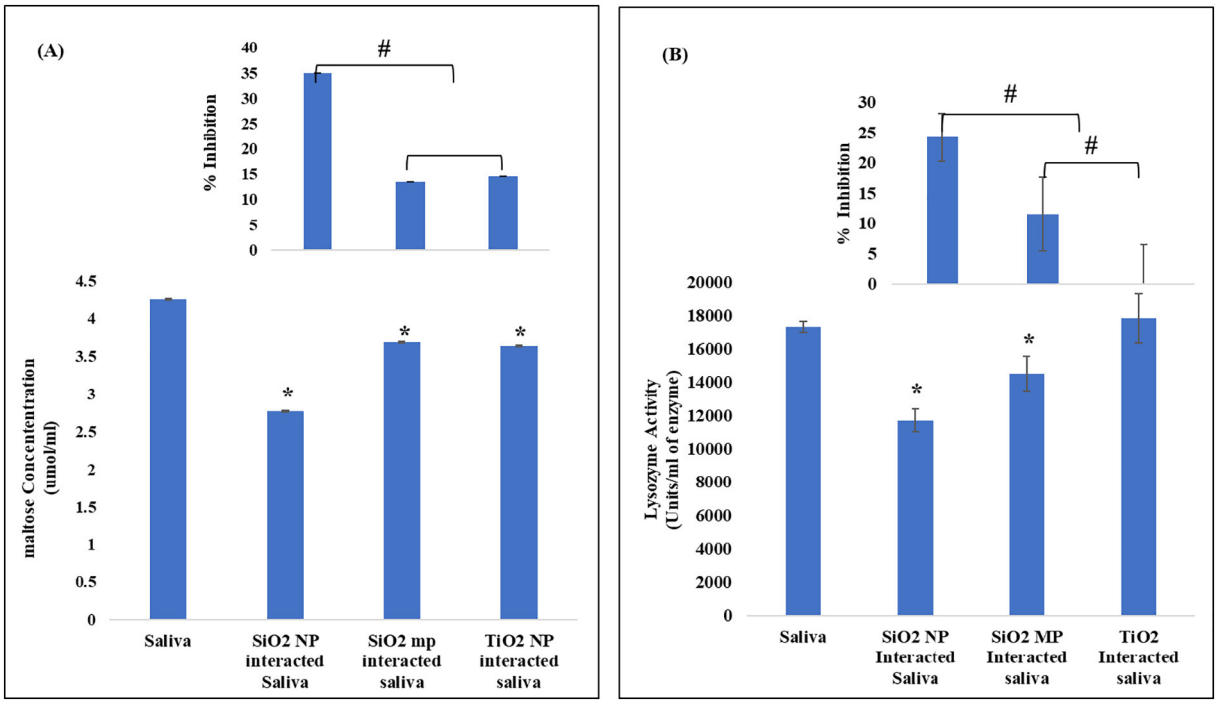

Fig. 7. Influence of dietary particles on the enzyme activity of α-amylase (A) and lysozyme in human saliva (B). α-Amylase activity was measured by DNS assay with particle concentration of 2 mg/mL. The enzyme inhibitory activity is expressed as decrease in units of maltose liberated. (B) Lysozyme activity was measured by turbidimetric method where *M. lysodeikticus* (bacterial model) cells suspended at 0.3 mg/mL were interacted with particles (1.25 mg/mL). Percentages of enzyme inhibitions are given in inlets. * and # indicate statistically significant difference from saliva control and between particles, respectively ($p \leq 0.05$).

interactions of particles with proteins could lead to compromised enzyme functions that are vital to the function of saliva. While the scope of this investigation was limited to understanding the interaction between pristine particles and human saliva, it should be noted that particles applied in food are likely to acquire surface coatings before they encounter saliva. Therefore, studies aimed at understanding the influence of food matrices on protein adsorption on particle surface and its effect on structure and function of vital salivary proteins are warranted for comprehending health effects ensuing ingestion of particles.

CRediT authorship contribution statement

Divya Srinivasan:Methodology, Investigation, Data curation, Writing - original draft.**Wut Hmone Phue**:Investigation, Writing - review & editing.**Ke Xu**:Investigation, Writing - review & editing.**Saji George**:Conceptualization, Supervision, Methodology, Formal analysis, Writing - review & editing.

Declaration of competing interest

The authors declare that they have no known competing financial interests or personal relationships that could have appeared to influence the work reported in this paper.

Acknowledgement

We thank Dr. Varoujan Yaylayan, Dr. Salwa Karboune, Dr. Yixiang Wang, Mr. Mazen Bahadi, and Mr. Horan Xing for technical support rendered during the course of this study. We acknowledge funding from NSERC RGPIN-2017-04727 and CRC/George/X-coded/248475 for supporting this research work.

Appendix A. Supplementary data

Supplementary data to this article can be found online at https://doi.org/10.1016/j.impact.2020.100238.

References

Ashburner, M., et al., 2000. Gene ontology: tool for the unification of biology. The gene ontology consortium. Nat. Genet. 25 (1), 25–29.
Barrán-Berdón, A.L., et al., 2013. Time evolution of nanoparticle–protein corona in human plasma: relevance for targeted drug delivery. Langmuir 29 (21), 6485–6494.
Bhushan, B., 2017. Introduction to nanotechnology. In: Springer Handbook of Nanotechnology. Springer, pp. 1–19.
Bihari, P., et al., 2008. Optimized dispersion of nanoparticles for biological *in vitro* and *in vivo* studies. Part. Fibre Toxicol. 5 (1), 14.
de Almeida, P.D.V., et al., 2008. Saliva composition and functions: a comprehensive review. J. Contemp. Dent. Pract. 9 (3), 72–80.
Deng, Z.J., et al., 2009. Differential plasma protein binding to metal oxide nanoparticles. Nanotechnology 20 (45), 455101.
Deng, Z.J., et al., 2012. Plasma protein binding of positively and negatively charged polymer-coated gold nanoparticles elicits different biological responses. Nanotoxicology 7 (3), 314–322.
Docter, D., et al., 2015. The nanoparticle biomolecule corona: lessons learned - challenge accepted? Chem. Soc. Rev. 44 (17), 6094–6121.
George, S., Kishen, A., 2007. Effect of tissue fluids on hydrophobicity and adherence of enterococcus faecalis to dentin. J. Endod. 33 (12), 1421–1425.
George, S., et al., 2012. Surface defects on plate-shaped silver nanoparticles contribute to its hazard potential in a fish gill cell line and Zebrafish embryos. ACS Nano 6 (5), 3745–3759.
Helal, R., Melzig, M., 2008. Determination of lysozyme activity by a fluorescence technique in comparison with the classical turbidity assay. Die Pharmazie-An International Journal of Pharmaceutical Sciences 63 (6), 415–419.
Hoebler, C., et al., 1998. Physical and chemical transformations of cereal food during oral digestion in human subjects. Br. J. Nutr. 80 (5), 429–436.
Hulla, J., et al., 2015. Nanotechnology: history and future. Hum. Exp. Toxicol. 34 (12), 1318–1321.
Humphrey, S.P., Williamson, R.T., 2001. A review of saliva: normal composition, flow, and function. J. Prosthet. Dent. 85 (2), 162–169.
Huynh, K.A., Chen, K.L., 2011. Aggregation kinetics of citrate and polyvinylpyrrolidone coated silver nanoparticles in monovalent and divalent electrolyte solutions. Environ. Sci. Technol. 45 (13), 5564–5571.
Ishihama, Y., et al., 2005. Exponentially modified protein abundance index (emPAI) for estimation of absolute protein amount in proteomics by the number of sequenced peptides per protein. Mol. Cell. Proteomics 4 (9), 1265–1272.
Jeon, Y.-M., et al., 2011. The effects of TiO 2 nanoparticles on the protein expression in mouse lung. Mol. Cell. Toxicol. 7 (3), 283.
Karmali, P.P., Simberg, D., 2011. Interactions of nanoparticles with plasma proteins:

implication on clearance and toxicity of drug delivery systems. Expert Opin. Drug Deliv. 8 (3), 343–357.
Ke, P.C., et al., 2017. A decade of the protein corona. ACS Nano 11 (12), 11773–11776 26.
Keller, A., et al., 2002. Empirical statistical model to estimate the accuracy of peptide identifications made by MS/MS and database search. Anal. Chem. 74 (20), 5383–5392.
Loo, J., et al., 2010. Comparative human salivary and plasma proteomes. J. Dent. Res. 89 (10), 1016–1023.
Lundqvist, M., et al., 2008. Nanoparticle size and surface properties determine the protein corona with possible implications for biological impacts. Proc. Natl. Acad. Sci. 105 (38), 14265–14270.
Mandel, A.L., Breslin, P.A., 2012. High endogenous salivary amylase activity is associated with improved glycemic homeostasis following starch ingestion in adults. J. Nutr. 142 (5), 853–858.
McCracken, C., et al., 2016. Critical assessment of toxicological effects of ingested nanoparticles. Environ. Sci. Nano 3 (2), 256–282.
Monopoli, M.P., et al., 2011. Physical− chemical aspects of protein corona: relevance to in vitro and in vivo biological impacts of nanoparticles. J. Am. Chem. Soc. 133 (8), 2525–2534.
Nesvizhskii, A.I., et al., 2003. A statistical model for identifying proteins by tandem mass spectrometry. Anal. Chem. 75 (17), 4646–4658.
Phue, W.H., et al., 2019. A comparative analysis of different grades of silica particles and temperature variants of food-grade silica nanoparticles for their physicochemical properties and effect on trypsin. J. Agric. Food Chem. 67 (44), 12264–12272.
Powell, J.J., et al., 2010. Origin and fate of dietary nanoparticles and microparticles in the gastrointestinal tract. J. Autoimmun. 34 (3), J226–J233.
Rashidi, L., Khosravi-Darani, K., 2011. The applications of nanotechnology in food industry. Crit. Rev. Food Sci. Nutr. 51 (8), 723–730.
Salih, E., et al., 2010. Large-scale phosphoproteome of human whole saliva using disulfide–thiol interchange covalent chromatography and mass spectrometry. Anal. Biochem. 407 (1), 19–33.
Sanfins, E., et al., 2011. Nanoparticle-Protein Interactions: From Crucial Plasma Proteins to Key Enzymes. Journal of Physics: Conference Series. IOP Publishing.
Schipper, R., et al., 2007. SELDI-TOF-MS of saliva: methodology and pre-treatment effects. J. Chromatogr. B 847 (1), 45–53.
Shevchenko, A., et al., 2007. In-gel digestion for mass spectrometric characterization of proteins and proteomes. Nat. Protoc. 1, 2856.
Tenzer, S., et al., 2011. Nanoparticle size is a critical physicochemical determinant of the human blood plasma corona: a comprehensive quantitative proteomic analysis. ACS Nano 5 (9), 7155–7167.
Tenzer, S., et al., 2013. Rapid formation of plasma protein corona critically affects nanoparticle pathophysiology. Nat. Nanotechnol. 8 (10), 772.
Treuel, L., 2013. How protein adsorption shapes the biological identity of NPs—where do we stand. J. Phys. Chem. Biophys. 3, e113.
van't Hof, W., et al., 2014. Antimicrobial defense systems in saliva. In: Saliva: Secretion and Functions. vol. 24. Karger Publishers, pp. 40–51.
Vertegel, A.A., et al., 2004. Silica nanoparticle size influences the structure and enzymatic activity of adsorbed lysozyme. Langmuir 20 (16), 6800–6807.
Walkey, C.D., Chan, W.C., 2012. Understanding and controlling the interaction of nanomaterials with proteins in a physiological environment. Chem. Soc. Rev. 41 (7), 2780–2799.
Winzen, S., et al., 2015. Complementary analysis of the hard and soft protein corona: sample preparation critically effects corona composition. Nanoscale 7 (7), 2992–3001.
Zanganeh, S., et al., 2018. In: Laurent, S. (Ed.), Chapter 3 - protein corona: the challenge at the nanobiointerfaces A2 - Mahmoudi, Morteza. Iron Oxide Nanoparticles for Biomedical Applications. Elsevier, pp. 91–104.